

Illumination of the subsurface towards identifying shadow zones and optimizing target images

Riaz Alai * (Petrotarget) and Jan Thorbecke (Delft University of Technology)

SUMMARY

Illumination analysis of wave propagation through the earth's subsurface is important for locating shadow zones and target prospects to optimize the success of exploration wells. Using illuminating beams for optimal data acquisition design and data processing provides a unique integrated and cascaded tool for optimal insight and interpretation of target prospects.

INTRODUCTION

Illuminating beams have been introduced by (Alá'i and Berkhout, 1996). In this abstract we use three dimensional illuminating beams for subsurface studies (Alai et al., 2007). Subsurface illumination plays an important role in the analysis and accuracy of migrated images and the overall detailed interpretation of the earth's subsurface (Alá'i, 1997). In the oil and gas industry, many complex algorithms are being developed to better image subsurface structures. However often it appears that specific necessary data has not been recorded during the "data acquisition" phase and any available migration or imaging algorithm will never produce the accurate image at desired target areas. To avoid unnecessary processing of data, insight and understanding of the shadow zones in measured data is crucial.

SUBSURFACE ILLUMINATION

To minimize the risk of dry wells, it is important to perform a detailed subsurface illumination analysis, followed by target-oriented processing. This method using illuminating beams in integrated data acquisition design and recordings followed by target-oriented processing will provide an accurate and controlled method for obtaining improved imaging of target structures in shortest possible time.

Subsurface illumination provides valuable information for

- Designing seismic data acquisition for a given subsurface model and target zone of interest.
- Using illumination energy to optimize migration algorithms for target-oriented imaging of target structures.

EXAMPLES

In this abstract, some examples will illustrate the importance of designing seismic data acquisition surveys based on a given subsurface model. The subsurface model used in this abstract is the salt model, issued from the joint SEG/EAGE 3-D Modeling Project (SEM). The SEG/EAGE salt model is one of the geological models that is used for modeling 3-D synthetic seismic datasets. The dimensions of the model are 13.5kmx13.5kmx4.2km. It has been built to address data quality issues encountered around the types of geological salt bodies in the Gulf of Mexico (Aminzadeh et al., 1995, 1996). The reflectors in the SEG/EAGE salt model are constructed by spikes positioned in a smoothly varying background (120% of the background velocity). The structure of the salt is presented with a high velocity of $C_p=4480\text{m/s}$ area. In the following examples a subset of the model has been used (6kmx6kmx4.2km). Figure 1 shows two vertical sections through the subset salt model.

In the following, an experiment is done by placing a source at a depth of $z=3820\text{m}$ and calculate the illumination from that source within the subset salt model (Thorbecke, 1997). Figure 2a shows an illuminating beam based on this point source in depth. The illuminating beam has been determined and integrated with the salt body in this figure. Figure 2b shows the illuminating beam without the integration of the salt body. Here it can be clearly observed that for that specific source point [and waves propagating through the complex salt model back to the earth's subsurface], two major curved patterns are recorded along the acquisition surface at $z=0\text{m}$. The acquisition surface can be better viewed in Figure 2c. This figure illustrates the illumination energy that has been recorded at the acquisition surface with various levels of amplitudes.

Figure 3a shows the illuminating beam superimposed on the subset salt model (vertical section along the lateral y direction) and Figure 3b illustrates the illuminating beam on a vertical section along the lateral x direction. Figure 3c shows the depth slice at depth $z=3820\text{m}$ in which the location of the point source can be observed.

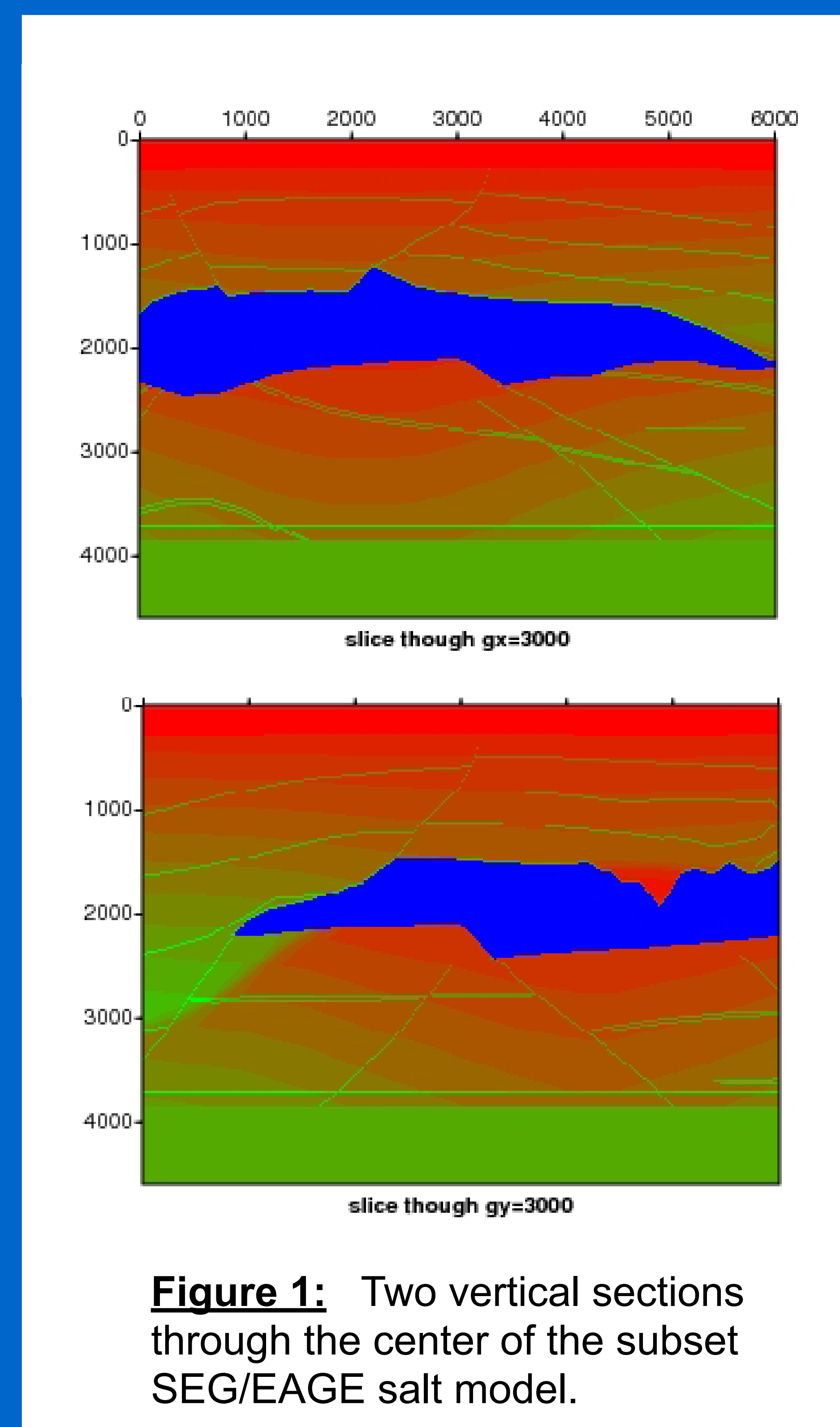


Figure 1: Two vertical sections through the center of the subset SEG/EAGE salt model.

Illumination of the subsurface towards identifying shadow zones and optimizing target images

Riaz Alai * (Petrotarget) and Jan Thorbecke (Delft University of Technology)

This example shows clearly that for that particular point source, some specific areas at the surface will be illuminated and can carry energy to the points of interest (other areas are considered shadow zones). Acquisition in the shadow zones does not capture energy from the point of interest.

In the following, another experiment is performed to better understand the illumination areas through the subset salt model. Figure 4a shows the target point at depth $z=3820\text{m}$, and Figure 4b illustrates the response at the acquisition surface (similar to Figure 2c). From this result of illumination, three point sources were selected at the surface along the illuminated areas of Figure 4b with highest energy values. Figure 4c shows the location of the three point sources at the surface level $z=0\text{m}$. Three illuminating beams have been calculated separately from these 3 point sources at the surface, and all resulting beams of these 3 point sources have been added together. Figure 4d shows a depth slices at depth $z=3820\text{m}$ from the added illuminating beams. From this figure, it can be noticed that some specific aligned areas, including our chosen target point, are being illuminated in the subsurface, and other areas are considered shadow zones in depth for those source combinations at the surface.

These examples show the importance of data acquisition design for optimally illuminating and imaging target structures (target-based data acquisition). On the other hand, illuminating beams can assist in optimizing target-oriented migration (acquisition-based imaging). This will avoid unnecessary processing of data.

In the following examples, one sail line has been selected over the subset salt model, and illuminating beams have been calculated for varying source distances along the sail line $x=3000\text{m}$. The experiments have been performed with varying source distances of 800m, 400m and 100m. Furthermore the illuminating beams have been calculated in which the salt body P-wave velocity has been replaced by salt body S-wave velocity. This velocity replacement has been done to observe the propagation and illumination difference between P-waves (longitudinal waves) and S-waves (transversal waves).

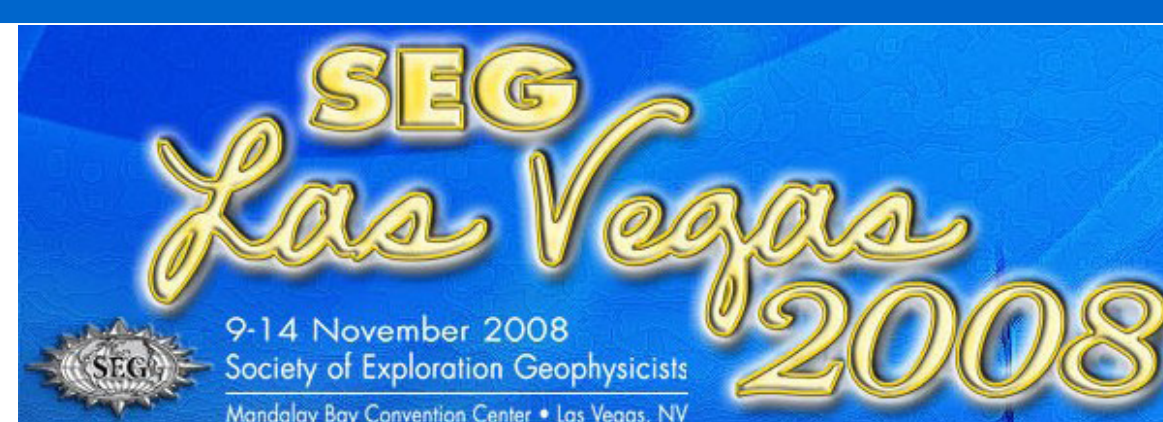
Figure 5a illustrates some of the surfaces of the SEG/EAGE salt model and other characteristics as seen in the Gulf of Mexico. The replacement of the P-wave salt body velocity is illustrated in Figure 5b and 5c. Figure 5b shows the subset salt model for which the salt body velocities are originally defined for P-wave propagation. Figure 5c shows the subset salt model, but in this model the salt body velocity has been replaced by S-wave velocity. Figure 6 shows the addition of illuminating beams for a varying number of shots along a sail line in the y-direction at $x=3000\text{m}$ (and using for P- or S-wave propagation velocities within the salt body). In Figure 6a, six pictures are depicted. The upper row shows vertical sections, for increasing number of sources, along the x-direction for illuminating beams through the model using the salt body P-wave velocity. The source distance is (from left to right) 800m, 400m, and 100m. Here it can be clearly observed that with increasing number of sources, a better illumination in the subsurface is obtained. The lower row of Figure 6a shows the same experiment, but in this case the salt body velocity has been replaced with the S-wave velocity in salt. Note the shadow zones and changes in energy in the various displays. It is clearly visible that S-waves which propagate through the salt body are much better suited for sub-salt imaging than P-waves. Strong wave conversions may occur at the interfaces of sediments and adjacent salt bodies. These wave conversions occur because of the high velocity contrasts and inhomogeneities, and in general P-waves get scattered, refracted and converted due the stronger wave distortion effects of P-waves at these strong velocity contrasts, yielding large shadow zones. On the other hand, the converted S-waves, propagate in general in the salt bodies with less wavefront distortion because of their lower propagation velocity and, therefore smaller contrasts with the surrounding sediment P-wave velocities. Figure 6b shows the results for slices along the y-direction. Figure 6c shows the depth slices of model illumination, with a source distance of 100m at depth level $z=2780\text{m}$. The left display shows the illumination of the propagation of P-waves through the salt. The right display shows the illumination of the propagating S-waves through the salt. Note the “shadow zones” and areas of poor illuminations.

CONCLUSIONS

Subsurface illumination studies are used to identify shadow zones in the data and facilitate the understanding of the limits in imaging. Subsurface illumination also indicates an optimal acquisition design given a specific area of interest. In this abstract it has been illustrated that S-waves, which have propagated through salt bodies, are much better suited for sub-salt imaging than P-waves.

REFERENCES

- Alá'i, R. and Berkhout, A.J., 1996, Generation of Pseudo VSP data from Common Focus Point gathers, 58th Annual EAGE Conference and Technical Exhibition, June 3-7, Amsterdam, The Netherlands, Extended Abstracts, Vol. 1, P135.
- Alá'i, R., 1997, Improving predrilling views by pseudo seismic borehole data: Ph.D. Dissertation, Delft University of Technology, Delft, The Netherlands, ISBN 90-9010768-1.
- Alai, R., Thorbecke, J. and Verschuur, D.J., 2007, Subsalt illumination studies through longitudinal and transversal wave propagation. 10th International Congress of the Brazilian Society, Rio de Janeiro, Brazil, 19-22 November 2007, B25.
- Aminzadeh, F., Burkhard, N., Kunz, T., Nicoletis, L., and Rocca, F., 1995, 3-D Modeling Project: 3rd report. The Leading Edge, Vol. 14, No. 2, 125-128.
- Aminzadeh, F., Burkhard, N., Long, J., Kunz, T. and Duclos, P., 1996, Three dimensional SEG/EAGE models - an update, The Leading Edge, Vol. 15, No.2, 131-134.
- Thorbecke, J., 1997, Common focus point technology: Ph.D. Dissertation, Delft University of Technology, Delft, The Netherlands.



SEG 2008 INTERNATIONAL EXPOSITION AND 78th ANNUAL MEETING, 9-14 NOVEMBER 2008, LAS VEGAS, NV



Illumination of the subsurface towards identifying shadow zones and optimizing target images

Riaz Alai * (Petrotarget) and Jan Thorbecke (Delft University of Technology)

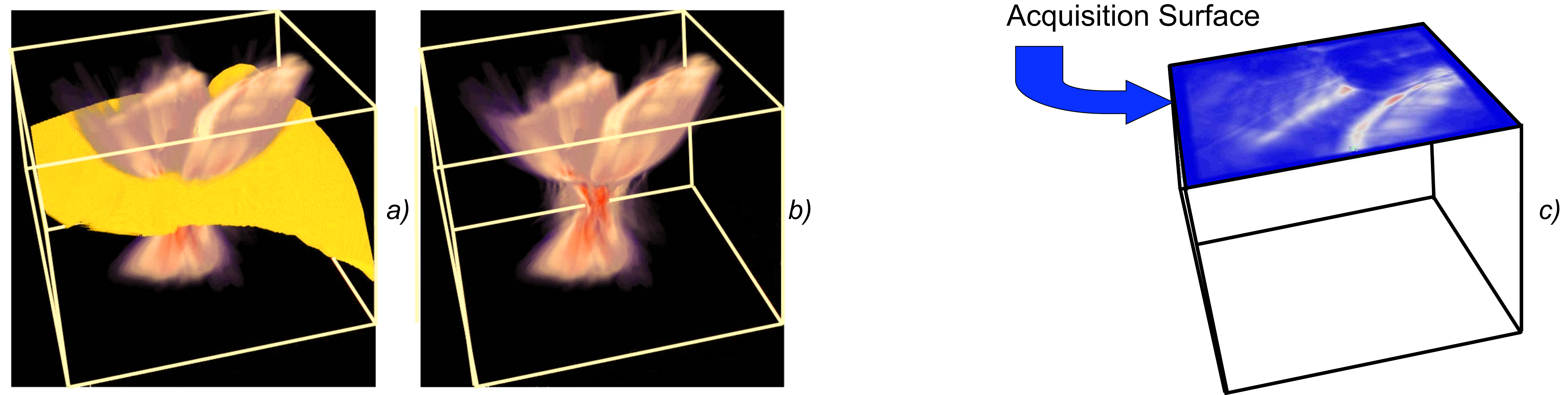


Figure 2: Illuminating beam for a point source in depth $z=3820\text{m}$ - a) integration of the salt body with beam, b) illuminating beam and c) acquisition surface showing the recorded energy that has arrived at the surface from the source point in depth

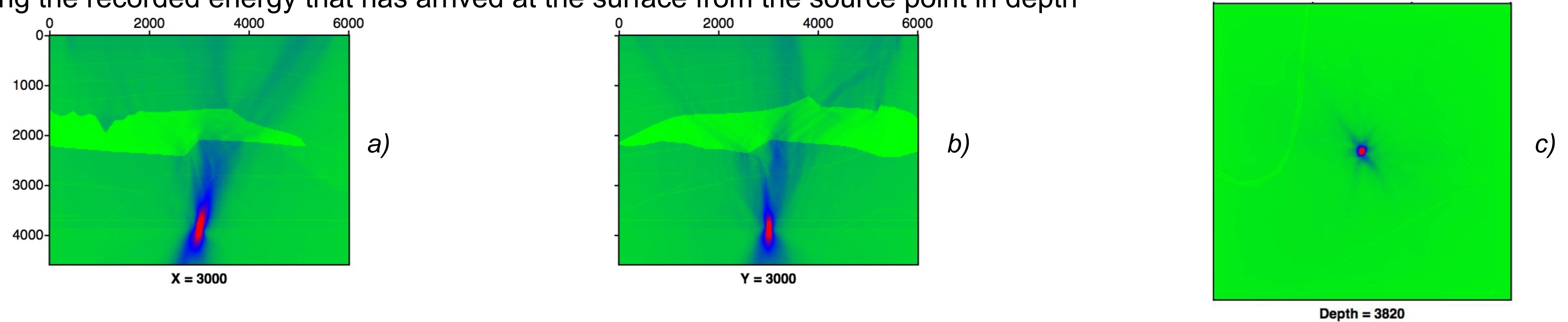


Figure 3: Illuminating beams superimposed on model, a) vertical section along y direction, b) vertical section along x direction and c) depth slice showing point source at depth $z=3820\text{m}$.

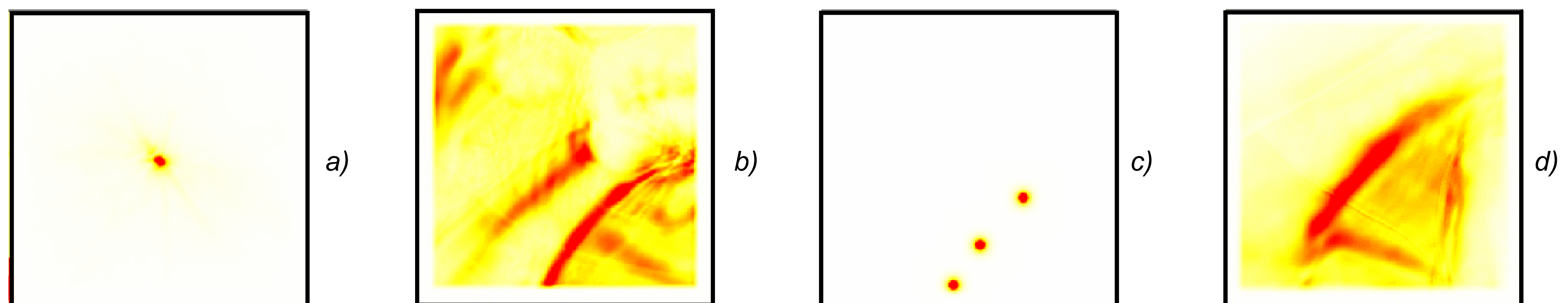


Figure 4: a) Point source at depth $z=3820\text{m}$, b) the determined energy at acquisition surface $z=0\text{m}$, c) 3 selected point sources at surface $z=0\text{m}$, and d) determined energy at depth slice $z=3820\text{m}$ (note the extended energy around the original target point at this depth).

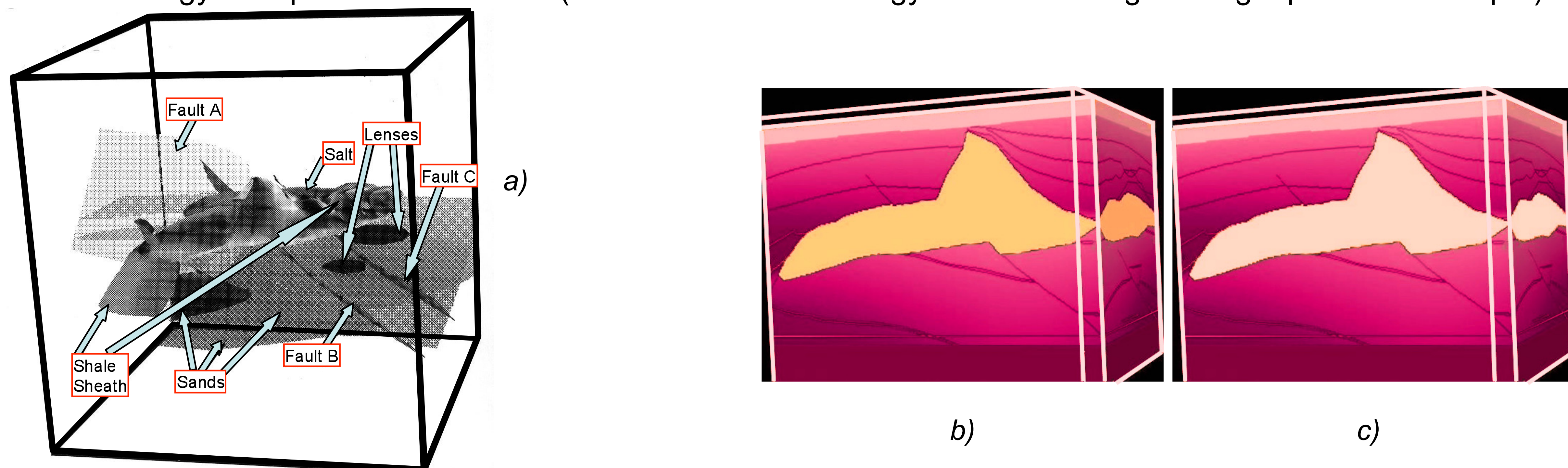


Figure 5: a) SEG/EAGE salt model, b) subset model, and c) subset model (salt body velocity has been replaced with S-wave velocity).

Illumination of the subsurface towards identifying shadow zones and optimizing target images

Riaz Alai * (Petrotarget) and Jan Thorbecke (Delft University of Technology)

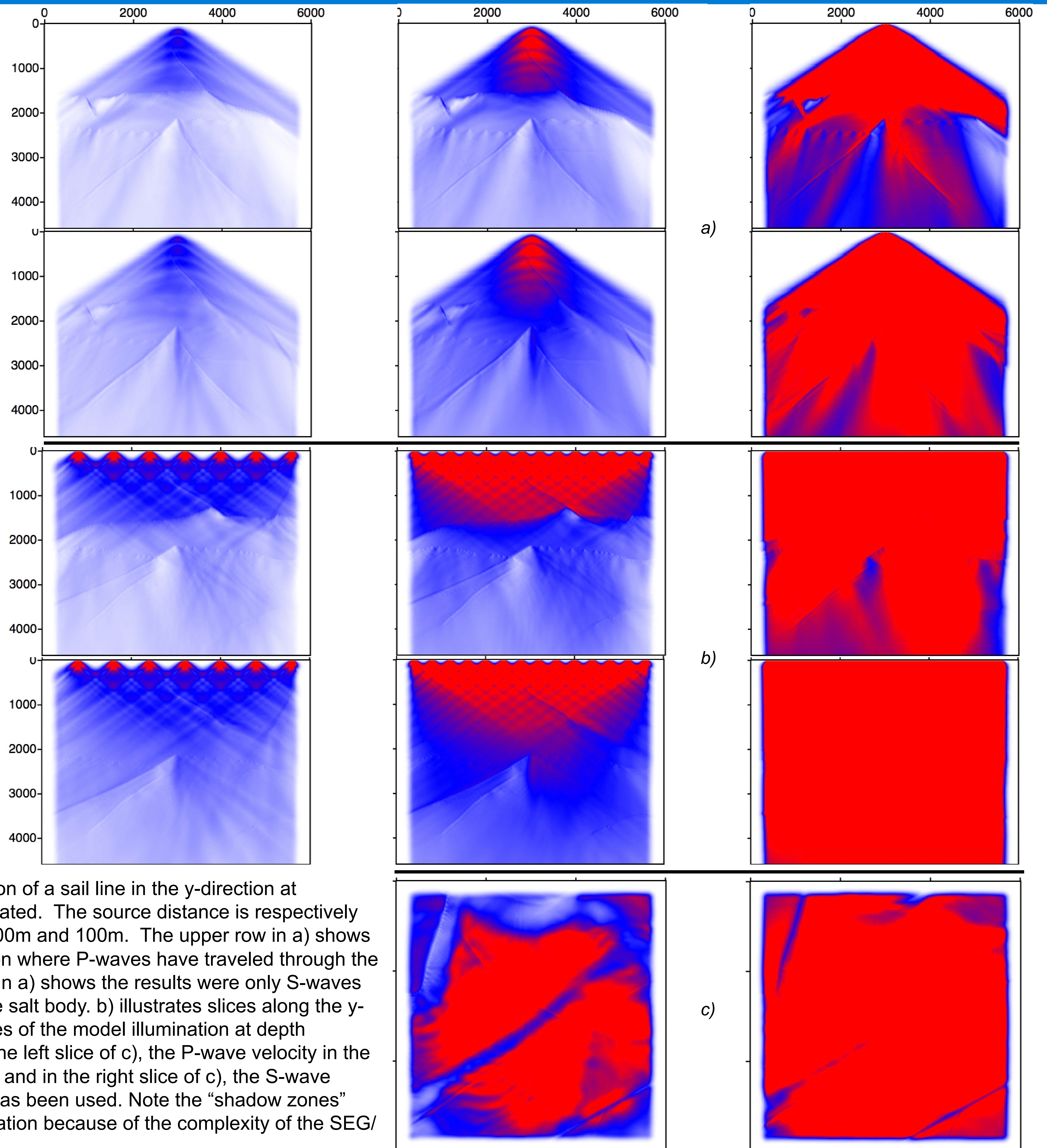


Figure 6: The illumination of a salt line in the y-direction at $x=3000\text{m}$ has been simulated. The source distance is respectively from left to right 800m, 400m and 100m. The upper row in a) shows slices along the x-direction where P-waves have traveled through the salt body. The lower row in a) shows the results were only S-waves have traveled through the salt body. b) illustrates slices along the y-direction. In c) depth slices of the model illumination at depth $z=2780\text{m}$ are shown. In the left slice of c), the P-wave velocity in the salt body has been used, and in the right slice of c), the S-wave velocity in the salt body has been used. Note the “shadow zones” and areas of poor illumination because of the complexity of the SEG/EAGE salt model.